# VI.G Cross-Cutting

## VI.G.1 Clean Energy Research*

*Dr. Ralph E. White*
*University of South Carolina*
*College of Engineering and Information Technology*
*Columbia, SC 29208*
*Phone: (803) 777-3270; Fax: (803) 777-6769; E-mail: white@engr.sc.edu*

*DOE Technology Development Manager: Carole Read*
*Phone: (202) 586-3152; Fax: (202) 586-9811; E-mail: Carole.Read@ee.doe.gov*

*DOE Project Officer: Paul Bakke*
*Phone: (303) 275-4916; Fax: (303) 275-4753; E-mail: Paul.Bakke@go.doe.gov*

*Contract Number: DE-FC36-04GO14232*

*Subcontractors:*
*Savannah River National Laboratory*
*South Carolina State University*

*Start Date: June 1, 2004*
*Projected End Date: November 30, 2005*

**Congressionally directed project*

### Objectives

The objectives of this work include:

- Advancing thermochemical hydrogen production processes.
- Studying the effect of metal dopants, carbon additive, and Al powder on the dehydrogenation and hydrogenation kinetics of complex metal hydrides (e.g., alanates) for on-board hydrogen storage.
- Investigating the gravimetric efficiency and kinetics of steam hydrolysis of sodium borohydride for on-board hydrogen storage and hydrogen production.
- Analyzing the effect of CO, $NH_3$, and $H_2S$ on fuel cell membrane electrode assembly durability.
- Developing mathematical models to characterize the performance and aging of fuel cell cathodes.

### Technical Barriers

This project addresses the following technical barriers from the Hydrogen, Fuel Cells and Infrastructure Technologies Program Multi-Year Research, Development and Demonstration Plan:

- Objective #1 addresses technical barriers associated the cost of hydrogen production.
- Objective #2 addresses the cost (A), weight and volume (B), durability (D), refueling time (E), hydrogen capacity and reversibility (M), and lack of understanding of hydrogen physisorption and chemisorption (N) barriers for the development of a viable on-board hydrogen storage system.
- Objective #3 addresses the on-board hydrogen storage technical barriers for weight and volume (B).

- Objective # 4 addresses the durability barrier associated with fuel cells.
- Objective #5 addresses the durability barrier and the cost barrier associated with fuel cells.

## Technical Targets

Objective 1 – These studies will be applied toward meeting the cost target for production of hydrogen from high-temperature thermochemical cycles of $3/gge.

Objective 2 – Comparison of DOE 2007 technical targets for on-board hydrogen storage systems with best to date (BTD) and soon to demonstrate (STD) research accomplishments is shown in the table below.

Technical Targets: On Board $H_2$ Storage System

| Storage Parameter | Units | 2007 Target | BTD[1] | STD[2] |
|---|---|---|---|---|
| gravimetriccapacity | kg $H_2$/kg sys | 0.045 | 0.03 (mat basis) | 0.05-0.06 (mat basis) |
| volumetric capacity | kg $H_2$/L sys | 0.036 | unknown[3] | unknown[3] |
| cost | $/kg $H_2$ | 200 | feasible[4] | viable[5] |
| operating temperature | °C | -20/50 | 100 | 80-90 |
| cycle life | # cycles | 500 | 500[6] | 500[7] |

[1] Based on the on-board regenerated metal-doped $NaAlH_4$ system.

[2] Based on the off-board regenerated $LiAlH_4$ system using the new physiochemical route for regeneration.

[3] No system yet, but could be an issue.

[4] Cost analysis possibly done for this system by DOE partners like Sandia National Laboratories; do not know where it falls relative to target.

[5] Cost analysis not done, but should be much cheaper than the Millennium Cell system, which makes it feasible.

[6] Thought to be possible, with large-scale cycling demonstrations either done or planned.

[7] Highly probably, based on new physiochemical route.

Objective 3 – Steam hydrolysis of $NaBH_4$ as-received (in powder form) gives high total yields (80% - 94%), but the present reaction configuration requires too much excess water. Hydrolysis of $NaBH_4$ thin films has better initial hydrogen generation rates and uses water more efficiently. Lower yields (~20% - 30%) have limited the specific energy obtained. We are working to increase the total yield of hydrogen from recrystallized thin films, projecting specific energies between 3.4% and 6.4%. The critical steps to obtain the FreedomCAR storage targets using steam hydrolysis of $NaBH_4$ are minimization of the amount of water required to obtain high yields of $H_2$ release, improvement of reactant contact to ensure all hydride is exposed to steam, and understanding the reaction mechanism and phase behavior of the steam hydrolysis of $NaBH_4$.

Comparison of experimentally observed values of usable specific energy for steam hydrolysis of $NaBH_4$ to DOE FreedomCAR targets is shown in the table below.

Usable Specific Energy from Hydrogen

| Year | 2007 | 2010 | 2015 | BTD* |
|---|---|---|---|---|
| Target (kg $H_2$/kg system) | 0.045 | 0.06 | 0.09 | 0.01 to 0.03 |

**BTD** = Best To Date or Current Value. *Values of 0.034 – 0.064 are projected to be feasible with improved reactant contact in recrystallized thin films of $NaBH_4$.

Objective 4 – Input from these studies will be applied toward meeting the durability target for stationary fuel cells of 40,000 hours (2010), and the cost target for stationary fuel cell stacks of $530/kWe.

Objective 5 – This project is conducting fundamental studies of the aging of fuel cell cathodes. Insights gained from these studies will be applied toward the design and synthesis of the polymer electrolyte membrane (PEM) fuel cell that meets the following DOE 2010 targets listed in Table 3.4.4 of the Multi-Year Research, Development and Demonstration Plan:

- Cost: $30/kW
- Durability: 5000 hours

## Approach

Our research on clean energy will be focused on hydrogen production, storage, and use in fuel cells. Our research plan consists of five projects with collaborations:

- Low-Temperature Electrolytic Hydrogen Production (Dr. John Weidner)
  - Investigate reverse Deacon process.
    - Obtain experimental current-voltage data on HCl and HBr electrolysis.
    - Develop model simulations of HCl and HBr electrolysis.
  - Develop model simulations that evaluate the performance of an electrolyzer for use in the hybrid sulfur cycle.
- Development of Complex Metal Hydride Hydrogen Storage Materials (Dr. James Ritter)
  - Develop new doped complex metal hydrides (alanates) that show reversible and cyclable hydrogen uptake and release.
  - Determine kinetics of hydrogen uptake/release.
- Hydrogen Storage Using Chemical Hydrides (Dr. Michael Matthews)
- Investigate the storage and retrieval of hydrogen from sodium borohydride ($NaBH_4$).
- Determine kinetics of the reaction between $NaBH_4$ and dry steam.
- Determine configuration of reactor and $NaBH_4$ that allows production of hydrogen in response to variable demand.
- Determine how reaction conditions affect hydrogen yield and water usage.
- Diagnostic Tools for Understanding Chemical Stresses and Membrane and Electrode Assembly (MEA) Durability Resulting from Hydrogen Impurities (Dr. John Van Zee)
  - Determine effects of impurities in $H_2$ on MEA durability.
  - Determine effects of CO.
  - Determine effects of $NH_3$.
  - Determine effects of $H_2S$.
- Durability Study of the Cathode of a PEM Fuel Cell (Dr. Ralph White)
  - Develop models to characterize the performance and ageing of the cathode in a PEM fuel cell.
  - Develop predictive models for cathode ageing and performance degradation.

## Results

<u>Objective #1 – Low-Temperature Electrolytic Hydrogen Production</u>

- The maximum current density achieved for the HCl electrolysis reaction for hydrogen generation was 12 $kA/m^2$ at voltages lower than 2 V.

- A reactor was built to electrolyze HCl to produce $H_2$, and hydrogen was generated from a PEM electrochemical reactor by electrolyzing HBr. The HBr reaction was successfully run in a PEM reactor, and the anhydrous conversion achieved a maximum of 20 $kA/m^2$ at 1.9 V.
- The conversion of $SO_2$ to $SO_3$ in a PEM electrolyzer was accomplished. The current density for this reaction at a potential of 0.835 V was 4 $kA/m^2$.

Objective #2 – Development of Complex Metal Hydride Hydrogen Storage Materials

- Discovered the synergistic effect of graphite on the dehydrogenation and hydrogenation kinetics of Ti-doped sodium aluminum hydride; patent application filed with the Savannah River National Laboratory (SRNL).
- Studied the synergistic effects of co-dopants such as Ti-Fe, Ti-Zr and Zr-Fe on the dehydrogenation kinetics of sodium aluminum hydride; a hypothesis has been proposed and is being verified.
- Studied the reversibility of hydrogen storage in novel complex hydrides such as Ti-doped lithium and magnesium aluminum hydrides; it was determined that these two complex hydrides are not reversible under the conditions in which sodium aluminum hydride easily reverses.

Objective #3 – Hydrogen Storage Using Chemical Hydrides

- Measured the hydrogen yield and apparent hydrogen kinetics using powder-form $NaBH_4$ and thin-film recrystallized $NaBH_4$; it is hypothesized that mass transfer and reactor design are key factors in the efficiency of the reaction.
- Developed a new reactor to investigate the mass transfer effects and help quantify intrinsic reaction kinetics.
- Determined water content and tentative structures of solid byproducts.

Objective #4 – Diagnostic Tools for Understanding Chemical Stresses and MEA Durability Resulting from Hydrogen Impurities

- Experiments completed to understand the effect of ionomer wt% in the catalyst layer on the rate of $NH_3$ poisoning of the anode. A kinetic analysis suggests that the reaction of $NH_3$ with the ionomer sites obeys a pseudo-first order reaction with a reaction rate constant of $k=1.2\ h^{-1}$.
- Methodology developed for 3-D predictions of degrading effects. Analysis of similarities and differences in concentration and dosage effects between data for CO for $NH_3$ and $H_2S$ completed. Model equations for $NH_3$ and $H_2S$ formulated.
- The degradation with $NH_3$ does not follow the same mechanism of competitive adsorption that is apparent with CO in $H_2$ mixtures.

Objective #5 – Developing Mathematical Models to Characterize the Performance and Aging of Fuel Cell Cathodes

- Confirmed the literature finding that the oxygen reduction reaction (ORR) exhibits a change in Tafel slope, e.g., at high cathode potential, the ORR exhibits a normal Tafel slope and at low cathode potential, a double Tafel slope.
- Demonstrated the need to include in the modeling of a polymer electrolyte membrane fuel cell a kinetic equation which has the ability to predict such Tafel slope change with cathode potential.
- Collected reliable rotating disk electrode (RDE) data over a wide range of temperatures, e.g., from 30 to 70ºC, and over a wide range of rotating speeds, e.g., from 400 to 3600 rpm.

## Future Directions

Objective #1 – Low-Temperature Electrolytic Hydrogen Production

- Mathematical models will be developed to predict the operation of PEM electrolyzers for the generation of hydrogen from HCl, HBr and $SO_2$.

Objective #2 – Development of Complex Metal Hydride Hydrogen Storage Materials

- Study the newly discovered sonochemical pretreatment method as a possible alternative to ball milling metal-doped alanates.
- Complete Raman study of Ti-doped $NaAlH_4$ with Dr. Williams.
- Continue to explore bimetallic and metal-carbon catalyzed alanates.
- Continue to work with Dr. Angerhofer at University of Florida on carrying out high field electron paramagnetic resonance studies with doped alanates.
- Continue to work with Dr. Rasolov at University of South Carolina on *ab initio* studies of $TiCl_3$-$NaAlH_4$ clusters, and initiate work with Dr. Delhomelle on *ab initio* studies of doped crystal structures.
- Continue to synthesize and study the reversibility of other metal-doped alanates and boronates, especially $LiAlH_4$ and $Mg(AlH_4)_2$, using the newly discovered physiochemical technique.

Objective #3 – Hydrogen Storage Using Chemical Hydrides

- Confirm the water content and crystal structure of byproducts of steam hydrolysis and verify the influence of these properties on the overall gravimetric efficiency of the reaction.
- Study the performance of the steam hydrolysis reaction using different reactor configurations and reactant preparations.
- Study hydrolysis of additional chemical hydrides ($LiB_4$, $NaAlH_4$, $MgH_2$, etc.).
- Increase reaction yields at higher temperatures in order to increase the efficiency of heat transfer in a prototype reactor.

Objective #4 – Diagnostic Tools for Understanding Chemical Stresses and MEA Durability Resulting from Hydrogen Impurities

- Use analysis and data obtained to predict distributions of poisons as a function of temperature, concentration, and dosage.
- Use predictions to calculate local stress resulting from hydrogen impurities.

Objective #5 – Developing Mathematical Models to Characterize the Performance and Aging of Fuel Cell Cathodes

- Develop a new ORR kinetic equation in place of the traditional Tafel equation to represent more accurately the potential-current relationship for a PEM cathode.
- Examine the kinetics for the hydrogen oxidation reaction (HOR) to evaluate the appropriateness of HOR models existing in the literature.
- Develop a new PEM fuel cell model which describes more accurately the potential-current relationship.

Objective #6, New for FY 2006 – Molecular Simulation of Hydrogen Storage Materials (co-PI Dr. Jerome Delhommelle)

- Model hydrogen storage in clathrate hydrates (Months 1-6).
- Model hydrogen storage in metal-organic frameworks (Months 7-12).
- Model hydrogen storage in doped single and multi-metal hydrides (Months 13-18).

## Objective #1: Low-Temperature Electrolytic Hydrogen Production

Thermochemical cycles produce hydrogen through a series of chemical reactions that result in the splitting of water at much lower temperatures (~800-1000ºC) than direct thermal dissociation (>2500°C) [1,2]. All other chemical species in these reactions are recycled, resulting in the consumption of only heat and water to produce hydrogen and oxygen. Since water rather than hydrocarbons is used as the source of hydrogen, no carbon dioxide emissions are produced and the hydrogen produced is highly pure.

Although there are hundreds of possible thermochemical cycles that can produce hydrogen from water, the two leading candidates are the sulfur-based cycles and the calcium-bromide-based cycles [3-5]. The sulfur-based processes all have the common oxygen-generating, high-temperature step, which is the decomposition of sulfuric acid to sulfur dioxide and oxygen at temperatures in the 850-1000ºC range. In the sulfur-iodine (S-I) cycle, the $SO_2$ is converted back to $H_2SO_4$ and hydrogen is produced via a two-step process involving iodine. The distillation of hydrogen iodide (HI) from solution and concurrent decomposition to iodine is the most difficult process issue for the iodine-containing portion of the cycle [4,5].

In the 1970s, Westinghouse Electric Corporation developed the hybrid sulfur process, which eliminated the use of iodine completely [6,7]. They electrochemically oxidized $SO_2$ to $H_2SO_4$ from a liquid-phase anode stream. Westinghouse demonstrated this process on a scale of 150 l/h of hydrogen in 1976, and a conceptual plant design has been developed.

The calcium-bromide-based cycles also have the potential of high efficiencies but with lower temperature requirements than the sulfur-based cycles (~750ºC). The common steps in these cycles are the conversion of CaO and $Br_2$ to $CaBr_2$ and $O_2$ at approximately 550ºC, and the conversion of $CaBr_2$ back to CaO and HBr at 730ºC. The second recycle step, converting HBr to $Br_2$ and generating hydrogen, can be done thermally in a solid-gas, fixed bed reactor of iron oxide, which in turn needs to be regenerated [4,5]. The iron reaction beds can be eliminated in a modified Ca-Br cycle by converting HBr directly to $Br_2$ and $H_2$ in a single step. This direct conversion can be performed electrochemically [8,9] or in a plasma process [10].

Aqueous-phase electrolysis suffers from (1) low current densities due to liquid-phase mass-transfer limitations and (2) difficult product separation due to dissolution of $Br_2$ in solution [8]. Gas-phase electrolysis has been attempted in phosphoric-acid [8,9] and molten-salt cells[10] to address these limitations. Although $Br_2$ dissolution was avoided in these cells, cell performance was poor.

In the PEM electrolyzer, $SO_2$ oxidation in the gas phase reduced the cell voltage by over 150 mV at 0.4 A/$cm^2$ compared to $SO_2$ oxidation in the liquid phase. This improvement was achieved with one-tenth the Pt loading. The process started to become mass-transfer limited at 0.4 A/$cm^2$ due to limitations in transporting water across the membrane above these currents. Further improvements maybe be possible by using thinner membranes, a humidified $SO_2$ feed stream, and elevated pressures.

In the HBr electrolyzer, dramatic improvements in current densities were achieved over previous gas-phase HBr electrolysis. Current densities were increased by over an order of magnitude (0.15 A/$cm^2$ to 2.0 A/$cm^2$) with no evidence of mass-transfer limitations. Future decreases in voltage while maintaining high current densities may be possible by using thinner membranes, more active catalysts, and elevated pressures.

## FY 2005 Publications and Presentations

1. P. Sivasubramanian, R. P. Ramasamy, C. E. Holland, F. Freire, and J. W. Weidner, "Electrochemical Generation of Hydrogen via Thermochemical Cycles," The American Institute of Chemical Engineers Spring Meeting, Atlanta, GA, April, 2005.
2. J. W. Weidner, P. Sivasubramanian, and F. Freire, "Electrochemical Recovery of $Cl_2$ from Anhydrous HCl Using a Polymer Electrolyte Membrane Reactor," The Electrochemical Society, Honolulu, HI, October, 2004.

3. J.W. Weidner, P. Sivasubramanian, and F. Freire, "Electrochemical Conversion of Anhydrous HBr to $Br_2$ for Hydrogen Production," The Electrochemical Society, Honolulu, HI, October, 2004.
4. P. Gomadam and J. W. Weidner, "Modeling Volume Expansion in Lithium-Ion Batteries," The Electrochemical Society, Honolulu, HI, October, 2004.
5. P. Sivasubramanian, R. P. Ramasamy, F. J. Freire, C. E. Holland and J. W. Weidner, "Electrochemical Hydrogen Production from Thermochemical Cycles Using a Proton Exchange Membrane Electrolyzer," Manuscript submitted for publication in the *International Journal of Hydrogen Energy*, 2005.

## References


1. M. A. Rosen, *Int. J. Hydrogen Energy,* 20, 7, 547 (1995).
2. National Academy of Engineering, "The Hydrogen Economy: Opportunities, Costs, Barriers, and R&D Needs," Chapter 8 (2004).
3. M. A. Rosen, *Int. J. Hydrogen Energy,* 21, 5, 349 (1996).
4. Nuclear Hydrogen R&D Plan DRAFT; Department Of Energy, Office of Nuclear Energy, Science and Technology, 2004.
5. Nuclear Hydrogen Initiative: Ten Year Program Plan, Office of Advanced Nuclear Research, DOE Office of Nuclear Energy, Science and Technology, March 2005.
6. P. W. Lu, E. R. Garcia and R. L. Ammon, *J. Appl. Electrochem.*, 11, 347 (1981).
7. P. W. Lu and R. L. Ammon, *J. Electrochem. Soc.,* 127, 2610 (1980).
8. W. Kondo, S. Mizuta, Y. Oosawa, T. Kumagai, and K. Fujii, "Decomposition of Hydrogen Bromide or Iodide by Gas Phase Electrolysis", *Bull. Chem. Soc. Jpn.*, **56**, 2504 (1983).
9. Y. Shimizu, N. Miura and N. Yamazoe, *Int. J. Hydrogen Energy*, **13**(6), 345 (1988).
10. C. N. Wauters and J. Winnick, *AIChE Journal*, 44(10), 2144-2148 (1998).


## Objective #2: Studying the Effects of Metal Dopants, Carbon Additive, and Al Powder on the Dehydrogenation and Hydrogenation Kinetics of Complex Metal Hydrides (e.g., alanates) for On-Board Hydrogen Storage

In one study [1], the synergistic effect of graphite as a co-dopant on the dehydrogenation and hydrogenation kinetics of Ti-doped $NaAlH_4$ has been observed for the first time. According to temperature-programmed desorption curves obtained at 2°C/min, the dehydrogenation temperature in the 90 to 150°C range decreased by as much as 15°C for $NaAlH_4$ co-doped with 10 wt% graphite (G) and up to 4 mol% $TiCl_3$ compared to similarly doped and ball milled samples without graphite. Constant-temperature desorption curves at 90 and 110°C obtained for $NaAlH_4$ co-doped with 2 mol% $TiCl_3$ and 10 wt% G also revealed improvements in the dehydrogenation kinetics of 6.5 and 3.0 times that of a similarly prepared sample without graphite, respectively. In contrast, graphite as a single dopant was essentially inactive as a catalyst. The effects of graphite persisted through dehydrogenation/hydrogenation cycling and through the addition of aluminum (Al) powder, which was added to mitigate irreversible kinetic and capacity losses during cycling. A sample of $NaAlH_4$ co-doped with 2.0 mol% $TiCl_3$, 10 wt% G and 5 wt% Al exhibited perhaps the best dehydrogenation and hydrogenation rates to date. The observed phenomena were interpreted in terms of some of the unique properties of graphite; graphite might be playing a dual role by serving as a mixing agent manifested through lubrication phenomena (i.e., graphene layer slippage and breakage), and as a micro-grinding agent manifested through the formation of carbide species, both during high-energy ball milling. In these capacities, graphite may have caused the Ti particles to be more finely ground and hence more dispersed over the surfaces of the $NaAlH_4$ particles and also the graphite particles themselves. Graphite might also be imparting an electronic contribution through the interaction of its facile π-electrons with Ti through a hydrogen spillover mechanism, whereby it back-donates some electrons to Ti, which further facilitates hydrogen bond formation and cleavage through this Ti species. Research is continuing with graphite as a co-dopant.

In another study [2], a systematic analysis of the effect of co-dopants on the dehydrogenation kinetics of freshly doped and ball milled $NaAlH_4$ samples was carried out with chlorides of Ti, Zr and Fe as the catalysts. Numerous samples of $NaAlH_4$, when co-doped with binary and ternary combinations of Ti, Zr and Fe at 4 mol% total catalyst content, exhibited synergistic behavior with respect to improving the dehydrogenation kinetics of the first decomposition reaction (i.e., $NaAlH_4 \rightarrow Na_3AlH_6$) over that of a sample of $NaAlH_4$ doped with 4 mol% Ti or Zr as single catalysts. In general, the dehydrogenation kinetics improved with the amount of Ti present in a co-doped sample, whether it was a binary or ternary system, with the top five performers all having at least 2 mol% Ti as one of the co-dopants. The binary combination of 3 mol% Ti – 1 mol% Fe exhibited the best synergistic performance, with dehydrogenation rates 3.7, 2.0 and 1.5 times that of 4 mol% Ti alone at 90, 110 and 130°C, respectively. The binary co-doped Zr-Fe systems exhibited more pronounced synergistic effects than did the binary co-doped Ti-Fe systems; however, their performance was always worse because Ti is a better single catalyst than Zr. The least synergism was exhibited by the binary co-doped Ti-Zr systems, and it was surmised that the superior electron sharing ability of electron-rich Fe was responsible for it being a better promoter of Ti and Zr than Zr was of Ti. This supposition was further supported by the systematic trends observed with the ternary co-doped systems, with their synergistic effects seemingly limited to binary combinations of the Ti-Fe and Zr-Fe systems. The effects of Ti, Zr and Fe as co-dopants on the second decomposition reaction (i.e., $Na_3AlH_6 \rightarrow NaH$) were not as pronounced as their effects on the first reaction, but synergisms were still observed, especially with all three binary Zr-Fe co-doped systems and to a lesser extent only with the 3 mol% Ti – 1 mol% Fe system. A future study will consider the effects of these co-dopants on the dehydrogenation/rehydrogenation kinetics after cycling.

In a third study [3], a comparison of the hydrogen release and uptake (cycling) capability of Ti-doped $NaAlH_4$, $LiAlH_4$ and $Mg(AlH_4)_2$ as a function of Ti dopant concentration, temperature, pressure, and cycle number is reported. Temperature-programmed desorption revealed hydrogen release capacities of around 3 wt% at 140°C, 3 wt% at 100°C and 6 wt% at 150°C, respectively, for the Ti-doped Na, Li and Mg alanates. In the same order, release capacities of 0.5, 2.0 and 1.5 wt% were obtained in 150, 6 and 150 min during constant-temperature desorption at 90°C. Although all three alanates exhibit striking characteristics that make them potential hydrogen storage materials, it remains that only Ti-doped $NaAlH_4$ exhibits around 3 wt% reversibility under reasonable conditions.

## Special Recognitions & Awards/Patents Issued

1. R. Zidan, J. A. Ritter, A. D. Ebner, J. Wang and C. E. Holland, "Hydrogen Storage Material and Process Using Graphite Additive with Metal Doped Complex Hydrides," Patent Application, U.S. Patent Application 2005/0032641A1 (2005).
2. J. Ritter, A. D. Ebner, C. H. Holland and T. Prozorov, "Method for Improving the Performance of Metal-Doped Complex Hydrides," Provisional Patent Application, filed February 28 (2005).

## FY 2005 Publications/Presentations

1. J. Wang, A. D. Ebner, T. Prozorov, R. Zidan, and J. A. Ritter, "Effect of Graphite on the Dehydrogenation and Hydrogenation Kinetics of Ti-Doped Sodium Aluminum Hydride," *J. Alloys and Compounds*, 395, 252-262 (2005).
2. J. Wang, A. D. Ebner, R. Zidan, and J. A. Ritter, "Synergistic Effects of Co-Dopants on the Dehydrogenation Kinetics of Sodium Aluminum Hydride," *J. Alloys and Compounds*, 391, 245-255 (2005).
3. J. Wang, A. D. Ebner and J. A. Ritter, "On the Reversibility of Hydrogen Storage in Novel Complex Hydrides," *Adsorption*, 11, 811-816 (2005).
4. J. Wang, T. Prozorov, A. D. Ebner and J. A. Ritter, "Novel Complex Hydrides for Reversible Hydrogen Storage," AIChE 2004 Annual Meeting, Austin, TX, November 2004, contributed.

## References

1. J. Wang, A. D. Ebner, T. Prozorov, R. Zidan, and J. A. Ritter, "Effect of Graphite on the Dehydrogenation and Hydrogenation Kinetics of Ti-Doped Sodium Aluminum Hydride," *J. Alloys and Compounds*, 395, 252-262 (2005).
2. J. Wang, A. D. Ebner, R. Zidan, and J. A. Ritter, "Synergistic Effects of Co-Dopants on the Dehydrogenation Kinetics of Sodium Aluminum Hydride," *J. Alloys and Compounds*, 391, 245-255 (2005).
3. J. Wang, A. D. Ebner and J. A. Ritter, "On the Reversibility of Hydrogen Storage in Novel Complex Hydrides," *Adsorption*, 11, 811-816 (2005).

## Objective #3: Studying the Reaction Kinetics, Reaction Products, and Mass Transfer Effects Associated with the Steam Hydrolysis of Solid $NaBH_4$ for On-Board Hydrogen Storage and Production

Data have been acquired in a tubular reactor using $NaBH_4$ either in powder form (as received) or recrystallized from ethylenediamine solution to form thin films. Table 1 shows hydrogen yields from the experiments at 110ºC for both powder form and thin-film reactant preparations. The addition of either methanol or acetic acid promotes higher yields of hydrogen. The experimental rates are lower than the theoretical rates, partially because of inefficient mass transfer. Examination of the reactor contents after the experiments revealed that the solid products were agglomerated. Presumably, the $NaBH_4$ on the surface of the particle reacts first and forms a layer of sodium borate ($NaBO_2$), which grows in thickness as the reaction proceeds. This layer retards steam diffusion through the $NaBH_4$ particle, decreasing the production of hydrogen. These experiments show mass efficiencies on a reactant basis [mass of liberated hydrogen / (mass of hydride + mass of $H_2O$ fed to the reactor)] of ~1.0 wt%, which is inefficient in terms of water utilization. This low water utilization is attributed primarily to the once-through passage of water vapor through the reactor. If the high yields associated with the powder-form $NaBH_4$ reaction (94%) can be realized with the recrystallized thin films, a specific yield of 3.4 kg $H_2$ per 100 kg of reactants can be predicted, assuming that the rates associated with the thin films remain close to the present values. If 100% yield is assumed at a constant production rate for thin films, a specific yield of 6.4 kg $H_2$ per 100 kg of reactants can be predicted. Additional reactor designs are being investigated in order to improve the reactant contact and water utilization. Unreacted water is recycled from the product in order to minimize the volume of water required for complete hydrolysis reaction.

**Table 1.** Data from Steam Hydrolysis of $NaBH_4$ from Tubular Reactor

| Reactant Preparation | Steam Composition | T (°C) | Max Slope (mol/min/$kg_{NaBH4}$) | % of Theo. $H_2$ Yield | Time (min) |
|---|---|---|---|---|---|
| $NaBH_4$ powder | Pure steam | 110 | 0.812 | 88.2 | 128 |
| $NaBH_4$ powder | Pure steam | 110 | 0.717 | 82.7 | 202 |
| $NaBH_4$ powder | 1% acetic acid | 110 | 0.582 | 101.4 | 228 |
| $NaBH_4$ powder | 1% methanol | 110 | 0.715 | 92.7 | 250 |
| $NaBH_4$ powder | Pure steam | 110 | 0.717 | 94.0 | 323 |
| $NaBH_4$ on glass beads | Pure steam | 110 | 4.01 | 19.7 | 29 |
| $NaBH_4$ on glass beads | Pure steam | 110 | 4.35 | 22.9 | 54 |
| Theoretical Rates | | x=0 | 11.1 | 100 | – |
| | | x=4 | 3.70 | 100 | – |
| | | x=6 | 2.78 | 100 | – |

The water content of the products is strongly related to the reaction mechanism and thus has an effect on the rate of hydrogen production and the specific yield. The crystal structure and degree of hydration of the products are studied using thermogravimetric analysis (TGA) and differential scanning calorimetry (DSC). The TGA scan of the reaction by-product is shown in Figure 1. The sample lost approximately 17% of its weight (free water and water of hydration) during the heating in the TGA. There are four inflection points that show different rates of water released, apparently due to changes in the hydration of $NaBO_2$. No weight loss occurred above approximately 275°C. The DSC scan in Figure 2 shows two peaks around 100°C and 150°C, which tentatively are ascribed to structural transformations from changes in the degree of hydration of the borate. The TGA and DSC scans improve understanding of the reaction pathway and will help understand how to minimize water consumption in the reactor.

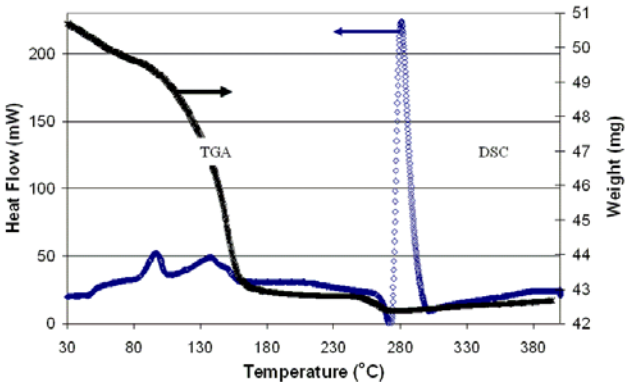


**Figure 1.** TGA and DSC of Product Material Extracted after Steam Hydrolysis of $NaBH_4$

## FY 2005 Publications/Presentations

1. Michael A. Matthews, Thomas A. Davis, and Eyma Y. Marrero-Alfonso, "Production of Hydrogen from Chemical Hydrides via Hydrolysis with Steam." *AIChE Annual Meeting*, Austin, TX (November 2004).
2. Michael A. Matthews, Thomas A. Davis, Joshua R. Gray, and Eyma Y. Marrero-Alfonso, "New Method for Hydrolysis from Chemical Hydrides." *The Annual Green Chemistry Conference*, Washington, D.C. (June 2005).
3. Michael A. Matthews, Thomas A. Davis, Joshua R. Gray, and Eyma Y. Marrero-Alfonso, "Challenges for Hydrogen Storage: Steam-Hydride Hydrolysis." *To be presented at the ACS National Meeting*, Washington, D.C. (August 2005).

## References

1. R. Aiello, J. H. Sharp and M. A. Matthews, "Production of Hydrogen from Chemical Hydrides via Hydrolysis with Steam," *Int. J. Hydrogen Energy*, 24, 1123-1130, 1999.

## Objective #4 – Diagnostic Tools for Understanding Chemical Stresses and MEA Durability Resulting from Hydrogen Impurities

Data were analyzed that show the effect of $NH_3$ impurities in reformate on the performance of Gore's advanced PRIMEA® Membrane Electrode Assembly (Series 5621) with reformate at 101 kPa and at 70°C. The steady-state polarization curves for different $NH_3$ concentrations (i.e., 80 and 200 ppm $NH_3$) in neat reformate (40% $H_2$, 17% $CO_2$, and 43% $N_2$) were measured and compared with a polarization curve for 500 ppm $NH_3$ in neat $H_2$. The polarization losses associated with $NH_3$ for neat hydrogen and neat reformate show that the current density decreased from 825 to 200 mA $cm^{-2}$ at 0.6 V when ammonia was introduced in the reformate. A cyclic transient test for 80 ppm $NH_3$ was performed to determine rates of poisoning and recovery. Electrochemical impedance spectroscopy (EIS) data are presented before, during, and after exposing the anode of the PEM fuel cell to $NH_3$ in an effort to characterize the poisoning and recovery. The membrane resistance, the intercept of Zreal at high frequency, only changes from 3.8 m before poisoning to 4.9 m after 10 hours exposure to 200 ppm $NH_3$ ($5.7x10^{-4}$ moles). For 500 ppm $NH_3$, these values are 3.8 m before poisoning to 5.2 m after 4 hours exposure. The impedance spectra was obtained with exposure of 200 ppm and 500 ppm $NH_3$ in neat $H_2$, keeping the dosage constant. The major findings include data that show that the steady-state polarization losses associated with $NH_3$ depend on the ratio of $NH_3$ partial pressure to $H_2$ partial pressure. The

same polarization curves were obtained with 200 ppm $NH_3$ in neat $H_2$ and with 80 ppm $NH_3$ in 40% $H_2$ with these "high-performance MEAs". Thus, there does not appear to be the same mechanism of competitive adsorption that is apparent with CO in $H_2$ mixtures.

Data were obtained to show the effect of ionomer loading on the anode electrode exposed to $NH_3$. Electrodes were prepared with 15%, 20%, and 25% Nafion® in the anode catalyst layer. These electrodes were studied at 200 ppm $NH_3$ in neat $H_2$ by recording changes in the cell voltage corresponding to a step change from neat $H_2$ to the $NH_3/H_2$ mixture while the current density was 0.6 A/cm$^2$. A model was developed to help understand which mechanism is controlling the decay of the cell performance. A kinetic analysis suggests that the reaction of $NH_3$ with the ionomer sites obeys a pseudo-first order reaction with a reaction rate constant of $k=1.2\ h^{-1}$.

## FY 2005 Publications/Presentations

1. Herie J. Soto, W-k. Lee, and J. W. Van Zee, "The Effect of Relatively High Ammonia Concentrations in Reformate on PEMFC Performance," submitted to Journal of Power Sources.
2. Herie J. Soto, V. A. Sethuraman, S. Greenway, and J. W. Van Zee, "The Effect of Ionomer Content on the Performance of a PEMFC Exposed to Ammonia," submitted to Journal of the Electrochemical Society.

## Objective #5 – Durability Study of the Cathode of a Polymer Electrolyte Membrane Fuel Cell

## Introduction

In the literature, the traditional Tafel equation has been almost exclusively used to describe the ORR kinetics in the modeling of a PEM fuel cell [1-6], regardless of the complexity of models. Unfortunately, the traditional Tafel equation can only be used to predict one value for the Tafel slope. This could create some uncertainty in evaluating the relative importance of other transport phenomena in the cathode, i.e., ionic (proton) conduction and dissolved $O_2$ diffusion in the catalyst layer, and $O_2$ diffusion and water transport in the gas diffusion layer, because it has been commonly observed from the RDE data that the ORR kinetics exhibits two Tafel slope values: a normal value for the Tafel slope at low overpotential (or high electrode potential) and a double value at high overpotential (or low electrode potential) [7-14]. To model the cathode of a PEM fuel cell, many people used in their Tafel equation a value similar to the one obtained at low overpotential for the Tafel slope [1-6]. As we know, the rate of voltage loss with current density is faster for a higher Tafel slope value. Therefore, it is not hard to imagine that, without the capability of predicting a Tafel slope change by the traditional Tafel equation, one or more transport processes will have to compensate for the underestimation of kinetics-induced faster voltage loss at high overpotentials. This will inevitably introduce some error in evaluating the significance of other transport processes. Due to the uncertainty in the exact mechanisms for the ORR kinetics [15], acceptable physics-based equations are not available in the literature. The objective of this work was to use a semi-empirical ORR kinetic equation, which is capable of predicting quantitatively the Tafel slope change with overpotential, to fit the RDE data collected in our lab. The RDE data collected in our lab were used in this work to determine parameter values. The goodness of fit using the empirical kinetic equation was compared with that using the traditional Tafel equation. Successful completion of this work will help improve the durability and cost targets for PEM fuel cells listed in the Multi-Year Research, Development and Demonstration Plan by providing an accurate modeling of fuel cell performance.

## Approach

The new ORR kinetic equation used to fit our RDE data has the form

$$i = -3c\frac{\psi}{c_{ref}}\left\{\sqrt{\frac{i_{ref}/c_{ref}}{\psi/c_{ref}}\exp\left(-\frac{2.3\eta}{b}\right)}\coth\left[\sqrt{\frac{i_{ref}/c_{ref}}{\psi/c_{ref}}\exp\left(-\frac{2.3\eta}{b}\right)}\right]-1\right\} \quad (1)$$

where $i$ is the kinetic current density of the ORR in the catalyst layer in A/cm$^3$, $i_{ref}$ is the exchange current density of the ORR in A/cm$^3$ at a reference concentration of dissolved $O_2$ equal to $c_{ref}$, is a fitting parameter and can be treated as a characteristic current density whose value determines the current density at which the Tafel slope of the ORR will double its value, $c$ is the concentration of dissolved $O_2$ in mol/cm$^3$, $b$ is the Tafel slope observed at low overpotentials, and is the overpotential of the $O_2$ electrode:

$$\eta = \Phi_1 - \Phi_2 - U^0 \tag{2}$$

where $_1$ and $_2$ are the solid and solution phase potentials of the catalyst layer, respectively, and $U^0$ is the standard equilibrium potential of the $O_2$ electrode evaluated relative to the standard hydrogen electrode (SHE). When is very small in magnitude, Equation 1 can be simplified to

$$i = -\frac{i_{ref}}{c_{ref}} c \exp\left(-\frac{2.3\eta}{b}\right) \tag{3}$$

which agrees exactly with the traditional Tafel equation. When is very large in magnitude, Equation 1 can be simplified to

$$i = -3\sqrt{\frac{\psi}{c_{ref}}}\sqrt{\frac{i_{ref}}{c_{ref}}} c \exp\left(-\frac{2.3\eta}{2b}\right) \tag{4}$$

which predicts the Tafel slope twice as large as does Equation 3. One may notice that Equation 1 has a form equivalent to those obtained after solving the diffusion equation for the dissolved $O_2$ in the catalyst agglomerate [4]. It is important to note that Equation 1 is introduced in this work only as an empirical kinetic equation, and it no longer carries any physical meaning associated with diffusion of $O_2$ in the agglomerate.

## Results

The RDE data (the diameter of the glassy carbon disk electrode is 4 mm, and the Pt loading is 24 $g_{Pt}/cm^2$) collected at 70°C are presented in Figure 1 over a wide range of rotating speeds, e.g., from 400 to 3600 rpm. By using the traditional Koutechy-Levich equation, the kinetic current density was extracted from the RDE data with a change in cathode potential, and it is presented in Figure 2. As seen in Figure 2, the relationship between the cathode potential and kinetic current density does not exhibit a single Tafel slope as predicted by the traditional Tafel equation. At high cathode potential (>0.8 V versus the standard hydrogen reference electrode), the Tafel slope has a value of 63 mV/decade (obtained using piece-wise fitting), and at low cathode potential (<0.75 V), the Tafel slope has a value of 128 mV/decade, which is approximately twice the value for the high potential region). Nonlinear least squares regression yields a value of 65.5 mV/decade for $b$ in Equation 1.

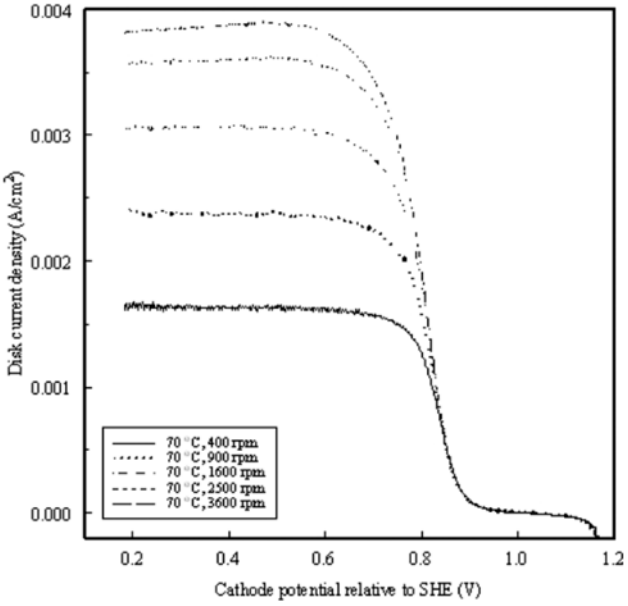


**Figure 1.** Experimental RDE Data Collected at 70ºC on a Glassy Carbon Disk Electrode with a Diameter of 4 mm. The disk current was normalized by the disk area (0.1257 cm$^2$) to yield the disk current density.

## Conclusions

It is concluded that the traditional Tafel equation is not as accurate as desired for predicting the relationship between the cathode potential and kinetic current density. Equation 1 can be used in place of the traditional Tafel equation with a desired accuracy.

## FY 2005 Publications/Presentations

1. Q. Guo, Q. Dong, L. Cao, Y. Tsou, E. De Castro, and R. E. White, "Using a semi-empirical equation to model the oxygen reduction kinetics", to be submitted to Journal of The Electrochemical Society.

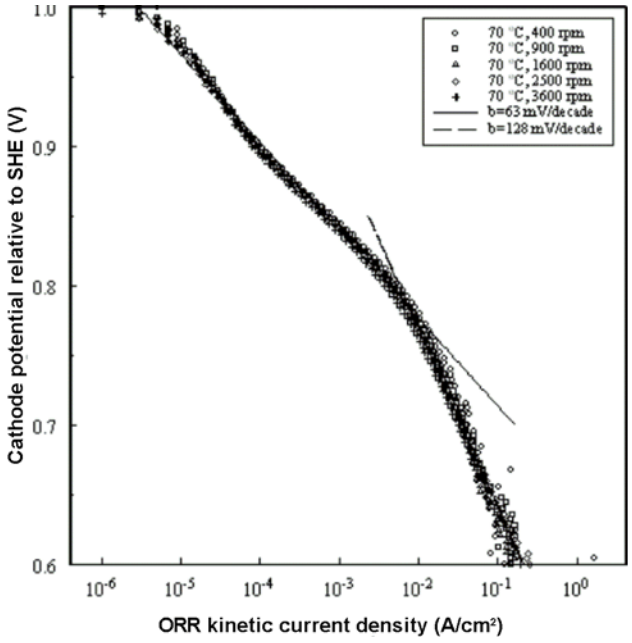


**Figure 2.** The Kinetic Current Density Extracted from the RDE Data Presented in Figure 1

## References

1. D. M. Bernardi, M. W. Verbrugge, *J. Electrochem. Soc.*, 139, 2477 (1992).
2. T. E. Springer, M. S. Wilson, S. Gottesfeld, *J. Electrochem. Soc.*, 140, 3513 (1993).
3. S. Um, C. Y. Wang, and K. S. Chen, *J. Electrochem. Soc.*, 147, 4485 (2000).
4. F. Jaouen, G. Lindbergh, G. Sundholm, *J. Electrochem. Soc.*, 149, 437 (2002).
5. G. Lin, W. He, and T. V. Nguyen, *J. Electrochem. Soc.*, 151, A1999 (2004).
6. A. Z. Weber and J. Newman, *J. Electrochem. Soc.*, 152, A677 (2005).
7. C. F. Zinola, A. M. Castro Luna, and A. J. Arvia, *Electrochimica Acta*, 39, 1951 (1994).
8. U. A. Paulus, T. J. Schmidt, H. A. Gasteiger, and R. J. Behm, *J. Electroanal. Chem.,* 495, 134 (2001).
9. U. A. Paulus, A. Wokaun, G. G. Scherer, T. J. Schmidt, V. Stamenkovic, N. M. Markovic, and P. N. Ross, *Electrochimica Acta*, 47, 3787 (2002).
10. V. S. Murthi, R. C. Urian, and S. Mukerjee, *J. Phys. Chem. B*, 108, 1011 (2004).
11. J. Shan and P. G. Pickup, *Electrochimica Acta*, 46, 119 (2000).
12. N. Wakabayashi, M. Takeichi, H. Uchida, and M. Watanabe, *J. Phys. Chem. B*, 109, 5836 (2005).
13. J. Jiang and B. Yi, *J. Electroanal. Chem.*, 577, 107 (2005).
14. S. Chen and A. Kucernak, *J. Phys. Chem. B,* 108*,* 3262 (2004).
15. N. A. Anastasijevic, V. Vesovic, and R. R. Adzic, *, J. Electroanal. Chem.,* 229, 305 (1987).